Microprocessor-Based Fuzzy Decentralized Control of 2-D Piezo-Driven Systems

Chih-Lyang Hwang, *Member, IEEE*

***Abstract*—In this paper, the trajectory tracking of a 2-D piezo-driven system (2DPDS) using microprocessor-based fuzzy decentralized control (MBFDC) is developed. It is known that the piezoelectric actuator contains hysteresis, which is not one-to-one mapping and memoryless nonlinearity. Due to this nonlinearity and the coupling characteristic of the 2DPDS, an effective decentralized control is difficult to design. From the very beginning, the suitable coefficients of switching surface are assigned to stabilize the dynamics of switching surface and to shape the response of tracking error. Based on the data of input/output, two scaling factors are employed to normalize the switching surface and its derivative. According to the concept of if–then rule, an appropriate rule table for the ith subsystem is then achieved. This table is skew symmetric about the diagonal line; the absolute value of this table is proportional to the distance to the diagonal line. According to the system stability, the output-scaling factor is determined. Finally, a sequence of experiments including the trajectory tracking using MBFDC, proportional–integral–differential control, and classic fuzzy control is carried out to confirm the usefulness of the proposed control system.**

***Index Terms*—Classic fuzzy control (CFC), decentralized control, fuzzy sliding-mode control (FSMC), microprocessor control, proportional–integral–differential (PID) control, 2-D piezo-driven system (2DPDS).**

I. Introduction

RECENTLY, ultrahigh precision manufacturing technology has become an important area, impacting on the production of high-density semiconductors, optical devices, and microelectromechanical systems/nanoelectromechanical systems. Micropositions of various operating principles have been devised: electromechanical, electrostatic, magnetostrictive, pyrelectric, piezoelectric, etc. Due to the improvement in the piezoceramic features (e.g., scale factor, linearity, and stability) and the inherent high resolution, the dominant type of micropositioner is piezoelectric [1]–[5]. Traditionally, the 2-D X–Y table system is driven by the motor with a ball screw [6]–[8], which possesses a narrow bandwidth and a frictional effect. Another approach for dual-axis system is Maglev guiding system [9]. However, its resolution is not fine, and the power consumption is larger than that of the piezo-driven system. Hence, the design and control of a 2-D piezo-driven system (2DPDS) are developed in this paper. The proposed control system contains a wide bandwidth, a low frictional effect, a fast response, and a high resolution.

Due to the hysteretic feature of piezoelectric actuator (PA), a controller based on a linear model is not enough for the trajectory tracking control of the PA. The past research work on control of the PA includes, for example, self-tuning control [10], feedforward control with proportional–integral–differential (PID) compensation [5], [11], and variable structure control [6], [12]. The proposed 2DPDS belongs to the nonlinear interconnected systems [4], [13]. Chang and Sun [4] use a feedforward and feedback control to reduce the effects of scale factor of nonlinearities, hysteresis, and output oscillations. It needs modeling and filtering to obtain an acceptable performance. This method is not a systematic approach; besides, a constant bias occurs. A recent paper developed by Perez *et al.* [13] discusses the modeling, fabrication, and validation of a 2DPDS with high performance. It requires thorough system knowledge to obtain an acceptable modeling. Its tracking performance is merely satisfactory. Due to the physical configuration and dimensionality of the 2DPDS, centralized control is neither economically feasible nor even necessary [14]. Due to the existence of nonlinear interconnections between two subsystems (e.g., frictional effect, nonlinear phenomenon of spring, and vibration of the X–Y table), there are not many efficient methods to deal with the high-frequency trajectory tracking control problem of the 2DPDS.

As one knows, a fuzzy control algorithm [15]–[18] consists of a set of heuristic decision rules and is regarded as a nonmathematical control algorithm, which has been proved to be very attractive whenever the controlled systems cannot be well defined or modeled. However, it needs a trial-and-error method to obtain an acceptable tracking performance. In addition to the heuristic-based fuzzy control, a model-based fuzzy control (e.g., the Takagi and Sugeno model-based control) is another approach to improve the performance of a fuzzy system [19], [20]. In this paper, the combination of sliding-mode control and fuzzy control, which is the so-called fuzzy sliding-mode control (FSMC), provides a robust controller for the nonlinear systems [21], [22]. The differences between the classic fuzzy control (CFC) and the FSMC are summarized as follows.

1) The coefficients of switching surface can shape the frequency of the closed-loop system; however, the CFC cannot possess this property.
2) Because the FSMC possesses the invariance property [23], disturbance immunity is better than that of the CFC, as the operating point is on the switching surface. In

Manuscript received October 19, 2006; revised July 30, 2007. This work was supported by the National Science Council of Taiwan, R.O.C. under Grant NSC-94-2213-E-036-003.

The author is with the Department of Electrical Engineering, Tamkang University, Tamsui 25137, Taiwan, R.O.C. (e-mail: clhwang@mail.tku.edu.tw).

Color versions of one or more of the figures in this paper are available online at http://ieeexplore.ieee.org.

Digital Object Identifier 10.1109/TIE.2007.907669

0278-0046/$25.00 © 2008 IEEE

Authorized licensed use limited to: Tamkang University. Downloaded on June 04,2010 at 03:28:46 UTC from IEEE Xplore. Restrictions apply.

TABLE I
RULE TABLE OF THE iTH FSMC

$\overline{s}_i$ \ $\dot{\overline{s}}_i$	PH	PB	PM	PS	PI	ZE	NI	NS	NM	NB	NH
NH	ZE	NI	NS	NM	NM	NB	NB	NB	NH	NH	NH
NB	PI	ZE	NI	NS	NM	NM	NB	NB	NB	NH	NH
NM	PS	PI	ZE	NI	NS	NM	NM	NB	NB	NB	NH
NS	PM	PS	PI	ZE	NI	NS	NM	NM	NB	NB	NB
NI	PM	PM	PS	PI	ZE	NI	NS	NM	NM	NB	NB
ZE	PB	PM	PM	PS	PI	ZE	NI	NS	NM	NM	NB
PI	PB	PB	PM	PM	PS	PI	ZE	NI	NS	NM	NM
PS	PB	PB	PB	PM	PM	PS	PI	ZE	NI	NS	NM
PM	PH	PB	PB	PB	PM	PM	PS	PI	ZE	NI	NS
PB	PH	PH	PB	PB	PB	PM	PM	PS	PI	ZE	NI
PH	PH	PH	PH	PB	PB	PB	PM	PM	PS	PI	ZE

short, the robustness of the FSMC is better than that of the CFC.

3) The adjustment of the control parameters for the FSMC is easier than that of the CFC. No trial-and-error method is needed.
4) The stability of the FSMC is easier and more systematic than that of the CFC.

The details of the aforementioned comparisons are described as follows. Property 1) is important because the bandwidth of the PA system is often high and because the unlimited bandwidth of the closed-loop system will cause an oscillating response and amplify the effect of disturbance. Property 2) can allude to the papers of sliding-mode control (e.g., [23]). Properties 3) and 4) are discussed as follows. There are *five* control parameters for the FSMC. It is easier to tune as compared with the CFC. Two coefficients are first set to obtain the suitable dynamics of the switching surface, which is the linear combination of present and past tracking error. Based on the practical ranges of the switching surface and its derivative, two normalizing scaling factors are selected. Finally, the fifth parameter is the output-scaling factor, which is chosen according to the system stability. Based on the Lyapunov stability of the closed-loop system, the fuzzy rule table of the ith subsystem using switching surface and its derivative (i.e., the set of if–then rules) is achieved, as shown in Table I. Due to the high demand of the PA system, the number of fuzzy rules is chosen large enough to obtain a fine tune of the control input. Then, the quantity of this fuzzy table is assigned as the value between -1 and 1 (see Table II). This table is skew symmetric about the diagonal line; its absolute value is proportional to the distance from the diagonal line. Then, the crisp control input, which is equal to the value determined from Table II, multiplying the output-scaling factor, is selected. Generally speaking, the larger the output-scaling factor assigned, the smaller the tracking error and the faster the response are; however, the risk of transient response occurs. Then, a saturation of control input will result in a possible instability.

TABLE II
LOOKUP TABLE OF THE iTH FSMC

$\overline{s}_i$ \ $\dot{\overline{s}}_i$	1.0	0.8	0.6	0.4	0.2	0	-0.2	-0.4	-0.6	-0.8	-1.0
-1.0	0.0	-0.1	-0.2	-0.4	-0.4	-0.7	-0.7	-0.7	-1.0	-1.0	-1.0
-0.8	0.1	0.0	-0.1	-0.2	-0.4	-0.4	-0.7	-0.7	-0.7	-1.0	-1.0
-0.6	0.2	0.1	0.0	-0.1	-0.2	-0.4	-0.4	-0.7	-0.7	-0.7	-1.0
-0.4	0.4	0.2	0.1	0.0	-0.1	-0.2	-0.4	-0.4	-0.7	-0.7	-0.7
-0.2	0.4	0.4	0.2	0.1	0.0	-0.1	-0.2	-0.4	-0.4	-0.7	-0.7
0	0.7	0.4	0.4	0.2	0.1	0.0	-0.1	-0.2	-0.4	-0.4	-0.7
0.2	0.7	0.7	0.4	0.4	0.2	0.1	0.0	-0.1	-0.2	-0.4	-0.4
0.4	0.7	0.7	0.7	0.4	0.4	0.2	0.1	0.0	-0.1	-0.2	-0.4
0.6	1.0	0.7	0.7	0.7	0.4	0.4	0.2	0.1	0.0	-0.1	-0.2
0.8	1.0	1.0	0.7	0.7	0.7	0.4	0.4	0.2	0.1	0.0	-0.1
1.0	1.0	1.0	1.0	0.7	0.7	0.7	0.4	0.4	0.2	0.1	0.0

Based on the concept of decentralized control, an FSMC is first applied to the individual subsystem of the 2DPDS. Until an acceptable tracking performance is accomplished, a *simultaneous* control of the 2DPDS is in progress. In this situation, a modified version of five control parameters is investigated to attain satisfactory responses for different reference trajectories in the presence (or absence) of payload. Another advantage of the proposed control is that the proposed controller design is independent of the reference trajectory, which does not necessarily belong to a specific category (e.g., step, ramp, and sinusoidal trajectory). The proposed control is simple and effective, as compared with the CFC. The proposed control algorithm can be easily implemented in a microprocessor [e.g., digital signal processor (DSP) of TMS320LF2407]. This paper is organized as follows. In Section II, the system description, system analysis, and problem formulation are given. In Section III, the design of the microprocessor-based fuzzy decentralized control (MBFDC) is discussed. Experiments comparing the PID control and the CFC, in the presence (or absence) of payload, and for a task assignment, are shown in Section IV. Finally, some concluding remarks are given in Section V.

II. SYSTEM DESCRIPTION, SYSTEM ANALYSIS, AND PROBLEM FORMULATION

A. System Description

Fig. 1 shows the experimental setup of the 2DPDS by the MBFDC. The 2DPDS consists of the following two main parts: 1) the piezomechanism, including carriage mechanism, position sensor, translator, and driver and 2) the microprocessor of TMS320LF2407 DSP from TI Company with the proposed MBFDC program written in C language.

The carriage mechanism, i.e., X–Y table, is made of steel for added strength. Four linear guides provided by THK Company (Model VRU3088) are used to support the moving part of the mechanism. Two sets of suitable springs with stiffness $k_{s_1} = 14.6$ kN/μm and $k_{s_2} = 23.1$ kN/μm are applied to preload the 2DPDS. The first PA system is Model P-246k023 from Physical Instrument (PI) Company. It is briefly described as follows: maximum expansion 120 μm, electric capacitance

Authorized licensed use limited to: Tamkang University. Downloaded on June 04,2010 at 03:28:46 UTC from IEEE Xplore. Restrictions apply.

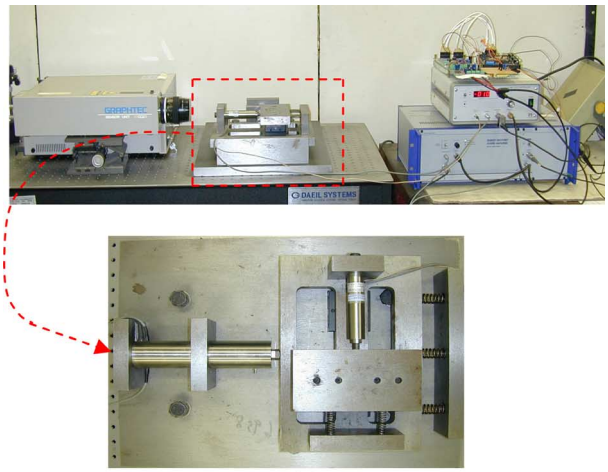

(a)

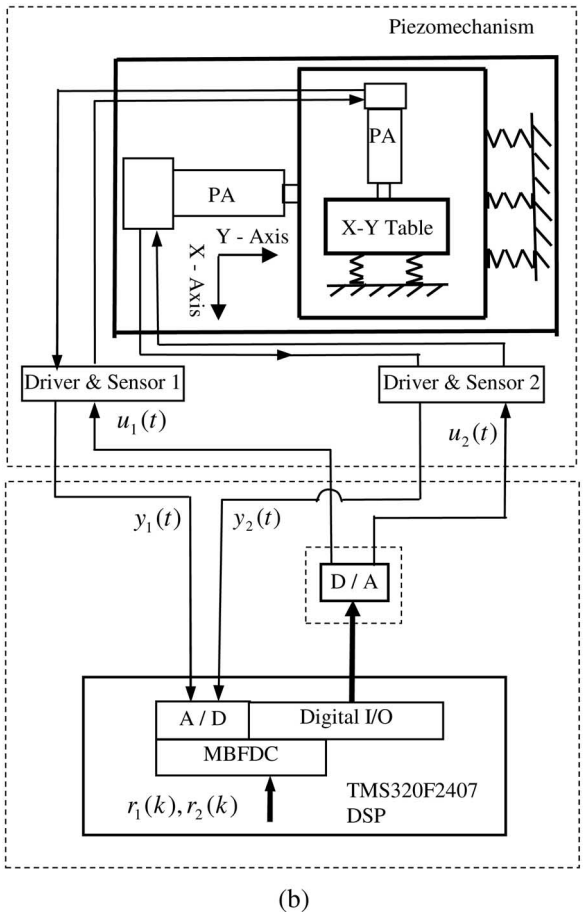

(b)

Fig. 1. Experimental setup of the 2DPDS by the MBFDC. (a) Photograph. (b) Block diagram.

3280 nF, stiffness 120 N/μm, and resonant frequency 3 kHz. The other PA system is Model P-845.40 from PI Company. Its main specifications are given as follows: maximum expansion 60 μm, electric capacitance 29 μF, stiffness 38 N/μm, and resonant frequency 5.5 kHz. The position signals $y_i(t), i = 1, 2$ are, respectively obtained by the position sensors, i.e., Model P-177.10 and Model P-176.60 of PI Company.

The hardware of the TMS320LF2407 DSP includes general purpose timers, analog/digital converter (ADC), full-compare PWM units, capture units, quadrature-encoder pulse,

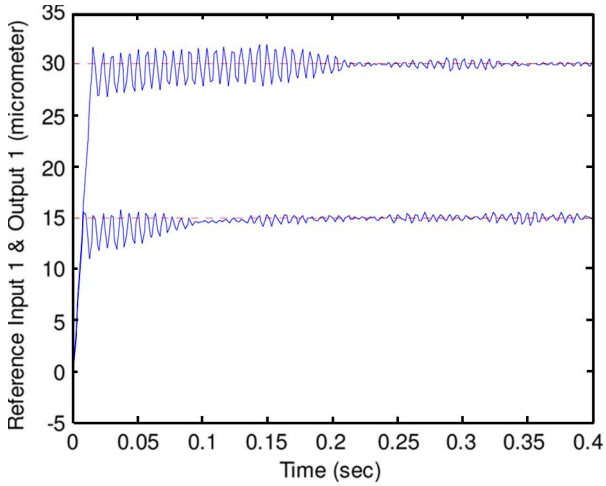

(a)

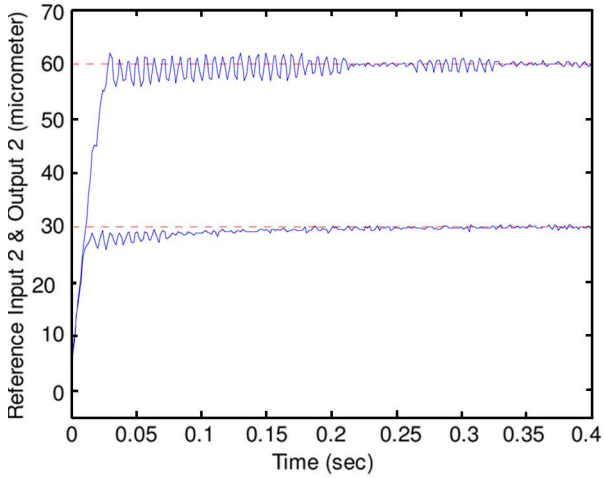

(b)

Fig. 2. Output responses $(-)$ of a PID control for the step reference trajectories $R(t) = [r_{m_1}, r_{m_2}]$ μm $(- - -)$. (a) $y_1(t)(-)$ for $r_{m_1} = 15$ μm and 30 μm $(- - -)$. (b) $y_2(t)(-)$ for $r_{m_2} = 30$ μm and 60 μm $(- - -)$.

series ports [e.g., series communication interface, series peripheral interface, control array network], and interface of joint test action group. Because the TMS320LF2407 DSP does not have a digital/analog converter (DAC), an interface using AD7541A, which is a 12-bit monolithic multiplying DAC from Analog Devices, is connected with digital input/output (I/O) of the DSP. The clock frequency of this DSP is 40 MHz.

These output signals of the PA systems are received by an analog-to-digital (A/D) interface of the TMS320LF2407 DSP. Together with a reference trajectory (i.e., $r_i(t)$, $i = 1, 2$), the control inputs $u_i(t)$, $i = 1, 2$ are calculated. The control inputs through digital-to-analog (D/A) interface are, respectively, sent to the drivers, which are Models E-507.00 and P-862.00 from PI Company. The output signals of the drivers are then applied to drive the two PAs. To reduce the effect of external disturbance, the aforementioned devices are all put on the $X-Y$ table with vibration isolation, i.e., model DVIO-I Series from Daeil Systems Company. The process is repeated until the total process time is over. The time required for every process is called the "control cycle time T_c". In this paper, 1.5 ms is used;

Authorized licensed use limited to: Tamkang University. Downloaded on June 04,2010 at 03:28:46 UTC from IEEE Xplore. Restrictions apply.

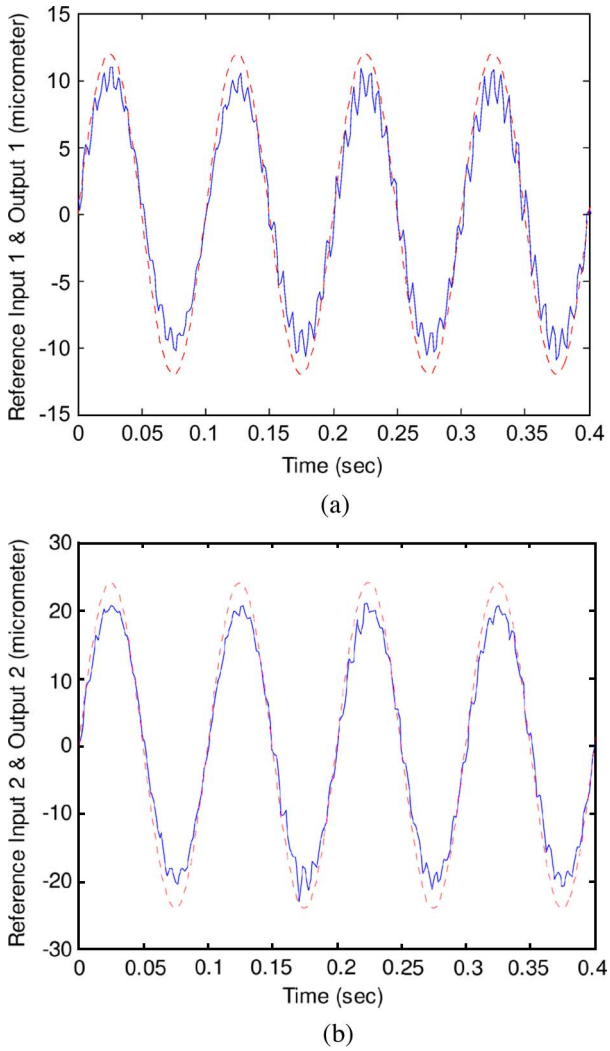

Fig. 3. Output responses $(-)$ of a PID control for the sinusoidal reference trajectories $R(t) = [\, r_{m_1} \sin(2\pi f_1 t) \quad r_{m_2} \sin(2\pi f_2 t)\,]\ \mu\text{m}\ (- - -)$. (a) $r_1(t)(- - -)$, $y_1(t)(-)$ for $f_1 = 10$ Hz, $r_{m_1} = 12\,\mu$m. (b) $r_2(t)$ $(- - -)$, $y_2(t)(-)$ for $f_2 = 10$ Hz, $r_{m_2} = 24\,\mu$m.

the sampling time of the ADC is also set as 1.5 ms. That is, the DSP executes two operations of the DAC and ADC for every 1.5 ms.

B. System Analysis

In the beginning, a PID control, as shown in the following equation, for the 2DPDS is investigated, as depicted in Figs. 2 and 3 whose responses are inferior:

$$u_i(k) = K_p\Big\{e_i(k) + T_c \sum e_i(k)/T_I + T_D\left[e_i(k) - e_i(k-1)\right]/T_c\Big\} \quad (1)$$

where $e_i(k) = r_i(k) - y_i(k)$. The control parameters for Figs. 2 and 3 are set as follows. For Fig. 2(a), $T_I = 0.05$, $T_D = 0.00005$, and $K_p = 4.0$ and (b) $T_I = 0.08$, $T_D = 0.00005$, and $K_p = 5.3$. For Fig. 3(a), $T_I = 0.05$, $T_D = 0.00005$, and $K_p = 4.2$ and (b) $T_I = 0.08$, $T_D = 0.00005$, and $K_p = 5.8$. The responses for the other parameters of PID control are similar to Figs. 2 and 3. For brevity, those are omitted. Due to the inferior performance of the 2DPDS by PID controls, an effective controller is required. This is the main motivation of this paper. The calibration of the 2DPDS is obtained through a laser vibrometer system—models AT3500 and AT0021 from Graphtec Company. The available measuring distance is from ± 5 to ± 40 mm for different conditions, the maximum sampling rate is 1.3 MHz, and the resolution of the measurement is 5 nm. Experimental results reveal that the position feedback signal of the PA can be represented as the position of the X–Y table after a suitable phase shift. For example, the shifts of the phase angle for the sinusoidal input with 10, 20, and 30 Hz are approximately equal to $3\pi/5$, $11\pi/5$, and $\pi/4$, respectively. For simplicity, these results are not shown.

C. Problem Formulation

From the very beginning, the FSMC achieved by the data of I/O and the stability requirement is constructed such that the tracking control of the 2DPDS is individually implemented. Although two subsystems of the 2DPDS are successfully and individually controlled by two FSMCs, the coupling effect and the unmodeled dynamics (e.g., frictional effect, nonlinear phenomenon of spring, and vibration of the X–Y table) of the 2DPDS always degrade the system performance. Based on our previous study (e.g., [21]), a modified version of scaling factors can improve the robust performance and robust stability. In general, there is a larger output-scaling factor, a smaller tracking error, and a greater satisfaction of inequality [e.g., (8)]. However, if a very large value of output-scaling factor is set, the risk of transient response occurs. Then, a saturation of the control input will result in an unstable status for the closed-loop system. Therefore, an appropriate output-scaling factor is very important such that the robust performance is accomplished. Eventually, the experimental results including 1) the MBFDC for different reference trajectories with (or without) payload and 2) the MBFDC for a specific motion of the 2DPDS are investigated; and 3) the trajectory tracking of the CFC is also investigated.

III. MBFDC

Consider the following 2DPDS (see, e.g., [2] and [3]):

$$A(Y)\ddot{Y}(t) + B(Y, \dot{Y}, t) = CU(t) \quad (2)$$

where $Y(t) \in \Re^2$ is the position of the 2DPDS, $A(Y) \in \Re^{2\times 2}$ denotes the inertia matrix of positive definite for any $Y(t)$, $B(Y, \dot{Y}, t) \in \Re^2$ comprises the nonlinearity and uncertainty of the system, $C \in \Re^{2\times 2}$ represents a control gain, and $U(t) \in \Re^2$ is the control input. It is assumed that the dynamics of (2) is *unknown*. However, the upper bound of function from (2) is supposed to be known. The fuzzy logic subsystem i in Fig. 4 performs a mapping from $X_i \in \Re^2$ to $\Re$. There are l fuzzy control rules and the upper script k denotes the kth fuzzy rule. Hence

$$\text{IF } \bar{s}_i(t) \text{ is } F_{1_i}^k \text{ and } \dot{\bar{s}}_i(t) \text{ is } F_{2_i}^k, \quad \text{THEN } \bar{u}_i(t) \text{ is } G_i^k \quad (3)$$

Authorized licensed use limited to: Tamkang University. Downloaded on June 04,2010 at 03:28:46 UTC from IEEE Xplore. Restrictions apply.

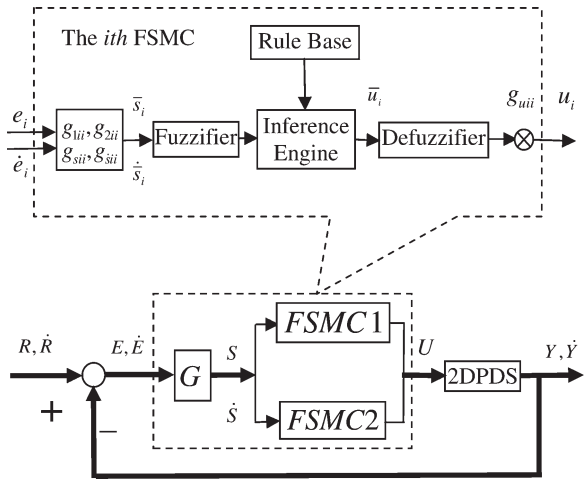

Fig. 4. Block diagram of the MBFDC.

where $x_i(t) = [\overline{s}_i(t) \quad \dot{\overline{s}}_i(t)]^T \in X_i \subset \Re^2$ and $\overline{u}_i(t) \in V_i \subset \Re$ are the input and output of the fuzzy logic subsystem i, respectively. $F_{j_i}^k (1 \le i, j \le 2, 1 \le k \le l)$ and G_i^k are labels of sets in X_i and V_i, respectively. The fuzzy inference engine performs a mapping from fuzzy sets in $X_i \subset \Re^2$ to fuzzy sets in $V_i \subset \Re$, which is based upon the fuzzy if–then rules in the fuzzy rule base and the compositional rule of inference. Let A_{x_i} be an arbitrary fuzzy set in X_i. The fuzzifier maps a crisp point $x_i(t)$ into a fuzzy set A_{x_i} in X_i. The center-average defuzzifier maps a fuzzy set in V_i to a crisp point in V_i. The corresponding five control parameters g_{1ii}, g_{2ii}, g_{sii}, $g_{\dot{s}ii}$, and g_{uii} are discussed later.

The proposed MBFDC includes two parallel FSMCs, and it has two switching surfaces shown as follows:

$$S(t) = GE(t) \quad G = [G_1 \quad G_2] \quad E(t) = \left[E_1^T(t) \quad E_2^T(t)\right]^T \tag{4}$$

where $S(t) \in \Re^2$, $G_1 = \mathrm{diag}(g_{1ii}) > 0$, $G_2 = \mathrm{diag}(g_{2ii}) > 0 \in \Re^{2\times 2}$, $i = 1, 2$ are the coefficients of the switching surface, and

$$E_1(t) = R(t) - Y(t) \quad E_2(t) = \dot{E}_1(t) \tag{5}$$

where $R(t) \in \Re^2$ is a reference trajectory, and $E_1(t) = [\, e_1(t) \quad e_2(t)\,]^T$. From (2) and (5), it leads to

$$\dot{E}_2(t) = \ddot{R}(t) - A^{-1}(Y)\left[CU(t) - B(Y, \dot{Y}, t)\right]. \tag{6}$$

The output of the MBFDC is designed as follows:

$$\begin{aligned} U(t) &= G_u \bar{U}(t) = G_u \left[GE(t) + \Delta \mathrm{sgn}(GE)\right] \\ &= G_u \left[S(t) + \Delta \mathrm{sgn}(S)\right] \end{aligned} \tag{7}$$

where $G_u = \mathrm{diag}(g_{uii}) > 0 \in \Re^{2\times 2}$ is the output-scaling factor, $\overline{U}(t)$ is fuzzy variable of $U(t)$, and $\Delta = \mathrm{diag}(\delta_{ii}) > 0 \in \Re^{2\times 2}$. It is also assumed that

$$g_{uii} \ge \{a_M c_M \left[|h_i(t)| + \lambda_i\right]\} / (g_{2m}\delta_{ii}), \qquad \text{for } i = 1, 2 \tag{8}$$

where $\lambda_i > 0$, $g_{2m} = \lambda_{\min}\{G_2\}$, $a_M = \lambda_{\max}\{A(Y)\}$, $c_M = \lambda_{\max}\{C\}$, and $h_i(t)$ is the ith element of the following matrix:

$$\begin{aligned} H(Y, \dot{Y}, \dot{R}, \ddot{R}) = G_1 &\left[\dot{R}(t) - \dot{Y}(t)\right] \\ &+ G_2 \left\{\ddot{R}(t) + A^{-1}(Y)B(Y, \dot{Y}, t)\right\}. \end{aligned} \tag{9}$$

The following theorem discusses the property of the MBFDC.

Theorem 1: Consider the unknown 2DPDS (2) with the known upper bound of (8). Applying (7) to system (2) gives the finite time to reach the switching surface (4), and the asymptotical tracking stability is obtained.

Proof: See the Appendix for a shrunken version of the proof. ■

Corollary 1: If inequality (8) is satisfied outside of the following convex set:

$$D = \{\, S(t) | \quad \|S(t)\| \le d_s \,\} \tag{10}$$

where d_s is a positive constant dependent on the upper bound of uncertainty, then the operating point reaches a convex set (10) in a finite time, and $\{S(t), U(t)\}$ are uniformly ultimately bounded.

According to the above discussions about the MBFDC for the 2DPDS (2), the design of the MBFDC is addressed as follows. Inequality (8) implies that the output-scaling factor should be greater than the upper bound of system gains, control gains, and uncertainty. Based on the I/O data, it is assumed that $\dot{s}_i(t)$ increases as $u_i(t) = g_{uii}\overline{u}_i(t)$ decreases, and if $s_i(t) > 0$, then increasing $u_i(t)$ will result in decreasing $s_i(t)\dot{s}_i(t)$, and if $s_i(t) < 0$, then decreasing $u_i(t)$ will result in decreasing $s_i(t)\dot{s}_i(t)$. That is, the control input $u_i(t)$ is designed in an attempt to satisfy the inequality $s_i(t)\dot{s}_i(t) < 0$, $i = 1, 2$, which result in the decrease of Lyapunov function $V(t) = \sum_{i=1}^{2} s_i^2(t)/2$, i.e., $\dot{V}(t) < 0$.

Due to the high demand of the trajectory tracking control of the PA system, the fuzzy variables $\overline{s}_i(t) = g_{sii}s_i(t)$ and $\dot{\overline{s}}_i(t) = g_{\dot{s}ii}\dot{s}_i(t)$, $i = 1, 2$ are quantized into the following 11 qualitative fuzzy variables (i.e., $l = 11$): 1) positive huge (PH); 2) positive big (PB); 3) positive medium (PM); 4) positive small (PS); 5) positive infinitesimal (PI); 6) zero (ZE); 7) negative infinitesimal (NI); 8) negative small (NS); 9) negative medium (NM); 10) negative big (NB); and 11) negative huge (NH). Note also that with the advantage of the proposed microprocessor, the storage for this arrangement is enough. There are many types of membership functions, some of which are bell shaped, trapezoidal shaped, and triangular shaped. The triangular type

Authorized licensed use limited to: Tamkang University. Downloaded on June 04,2010 at 03:28:46 UTC from IEEE Xplore. Restrictions apply.

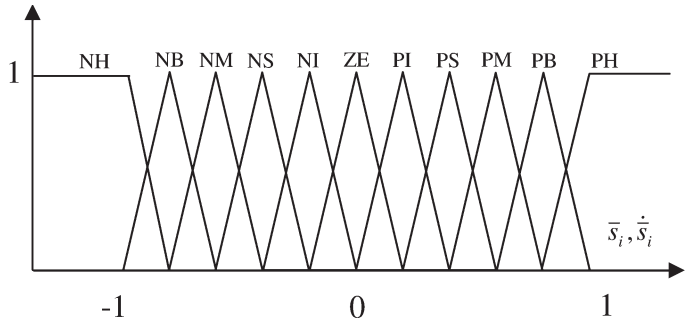

Fig. 5. Membership functions with triangular type.

in Fig. 5 is used in this paper. In summary, the linguistic rule of the ith MBFDC is shown in Table I by which the center of the gravity method is employed to form a lookup Table II that directly relates the inputs $\overline{s}_i(t)$ and $\dot{\overline{s}}_i(t)$ with the output $\overline{u}_i(t)$. The control actions of the diagonal terms in Table II are ZE. This arrangement is similar to a sliding-mode controller that has a switching surface. In addition, the control actions of the upper triangle terms are from NI to NH, and those of the lower triangle terms are from PI to PH. It is skew symmetric. The proposed control algorithm is easily implemented in the TMS320LF2407 DSP from TI Company, which is the so-called "microprocessor-based" control.

Finally, the guideline for the selection of the five control parameters is addressed as follows. 1) Based on inequality (8), the output-scaling factor g_{uii} is assigned. In the beginning, it is chosen from a small value. According to the response, a larger value is then applied to improve the system performance. When a larger output-scaling factor is selected, a smaller tracking error is achieved; however, the risk of transient (or unstable) response occurs due to the constraints of the (rate of) control input. 2) The parameters g_{sii} and $g_{\dot{s}ii}$ are chosen such that $\overline{s}_i(t)$ and $\dot{\overline{s}}_i(t) \in [-1, 1]$. 3) The dynamics of the switching surface should not be faster than that of reaching phase. That is, $-\lambda\{g_{1ii}/g_{2ii}\} < cg_{uii}$, where c is a suitable and positive constant. 4) The smaller the $-\lambda\{g_{1ii}/g_{2ii}\}$ is set, the narrower the bandwidth of the switching surface is assigned. Then, the higher frequency component of the tracking error is filtered. However, the response of the trajectory tracking becomes more sluggish (refer to Section IV).

IV. Experimental Results

This section is divided in two: one discusses the trajectory tracking of the 2DPDS using the MBFDC, and the other examines the task assignment using the 2DPDS by the MBFDC.

A. Trajectory Tracking of the 2DPDS Using the MBFDC

In the beginning, the experiments for the individual subsystem are investigated. Until an acceptable performance for every subsystem is achieved, the simultaneous motion of the 2DPDS is investigated. For brevity, the responses for an individual subsystem are omitted. Fig. 6 shows the response of the 2DPDS for different step reference trajectories by the following control parameters: $G_1 = I_2$, $G_2 = \mathrm{diag}\{287.2, 237.8\}$, $G_s = \mathrm{diag}\{1, 1.06\}$, $G_{\dot{s}} = \mathrm{diag}\{120, 66.7\}$, and $G_u = 1.6I_2$. The selection of G_1 and G_2 ensures that the bandwidths of the switching surface for subsystems 1 and 2 are, respectively, 45.7 and 37.9 Hz. Therefore, the responses for the step reference trajectories can be without overshoot, which are much better than that of Fig. 2 using a PID control. A very wide bandwidth will cause an oscillating response; a very narrow bandwidth will make the response sluggish. Hence, a compromise should be made. On the contrary, the CFC does not have this feature. The corresponding responses of Figs. 2 and 3 using CFC are oscillatory. For simplicity, those are omitted. This is the reason why the output responses using the proposed control [i.e., Fig. 6(a) and (d)] are smooth. It is the contribution of this paper to provide an effective controller for the 2DPDS. The control inputs for these step reference trajectories are depicted in Fig. 6(b) and (e), which are smooth enough. The responses of the switching surface are also in the neighborhood of $s_i = 0$, $i = 1, 2$ [see Fig. 6(c) and (f)]. Although the response of the switching surface is chattering, the suitable G_1 and G_2 can filter the high-frequency component of s_i, $i = 1, 2$ so that the tracking error (or output) is smooth. It indicates that the proposed control indeed fulfills the design goal. The maximum steady-state tracking error is also shown in Table III, which is acceptable.

For further verification of the usefulness of the proposed control, the responses for the sinusoidal reference trajectories $R(t) = [\, r_{m_1} \sin(2\pi f_1 t) \quad r_{m_2} \sin(2\pi f_2 t\,)]$ μm, with f_1, $f_2 =$ 5, 10, 20 Hz, $r_{m_1} = 12$ μm, and $r_{m_2} = 24$ μm, are examined. The control parameters of Fig. 7 are the same as that of Fig. 6 except $G_2 = \mathrm{diag}\{496.3, 383.6\}$. It reveals that the bandwidths of the switching surface for subsystems 1 and 2 are 79 and 61.1 Hz, respectively. The reason for choosing these bandwidths is that the sinusoidal reference trajectory is already smooth, and its frequency is up to 20 Hz. The bandwidth of the switching surface must be large enough to track a higher frequency trajectory. Otherwise, a *phase* tracking error will occur. Although a larger bandwidth can obtain an acceptable tracking result for the high-frequency reference trajectory, this situation probably amplifies the effect of the high-frequency disturbance. The control inputs for these sinusoidal reference trajectories are smooth; the responses of the switching surface are also in the vicinity of $s_i = 0, i = 1, 2$. Similarly, the suitable G_1 and G_2 can filter the high-frequency component of s_i,

Authorized licensed use limited to: Tamkang University. Downloaded on June 04,2010 at 03:28:46 UTC from IEEE Xplore. Restrictions apply.

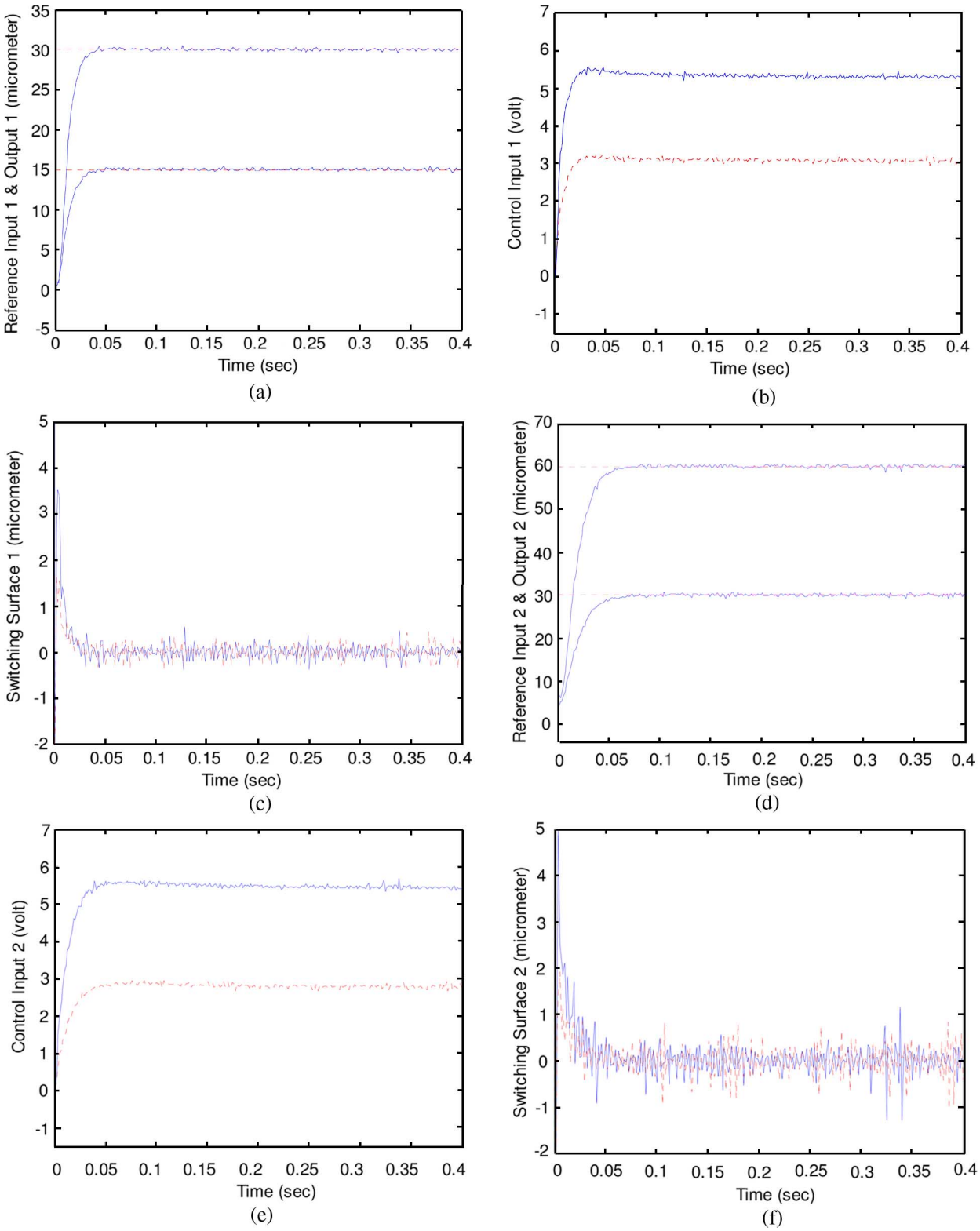

Fig. 6. Responses $(-)$ of the MBFDC for the step reference trajectories $R(t) = [r_{m_1}, r_{m_2}]$ μm $(- - -)$. (a) $(y_1(t)$ $(-)$ for $r_{m_1} = 15$ μm and 30 μm $(- - -)$. (b) $u_1(t)$ for $r_{m_2} = 15$ μm $(- - -)$ and 30 μm $(-)$. (c) $s_1(t)$ for $r_{m_2} = 15$ μm $(- - -)$ and 30 μm $(-)$. (d) $y_2(t)$ $(-)$ for $r_{m_2} = 30$ μm and 60 μm $(- - -)$. (e) $u_2(t)$ $(-)$ for $r_{m_2} = 30$ μm and 60 μm $(- - -)$. (f) $s_2(t)$ for $r_{m_2} = 30$ μm $(- - -)$ and 60 μm $(-)$.

$i = 1, 2$, so that the tracking error (or output) is smooth. Due to the space constraint, only the output response of 20 Hz is presented in Fig. 7. Furthermore, the corresponding maximum steady-state tracking errors of the aforementioned cases are depicted in Table III. It reveals that the higher the frequency of the reference trajectory, the greater the chance that

Authorized licensed use limited to: Tamkang University. Downloaded on June 04,2010 at 03:28:46 UTC from IEEE Xplore. Restrictions apply.

TABLE III
MAXIMUM STEADY-STATE TRACKING ERROR WITH ABSOLUTE VALUE IN MICROMETERS AND RELATIVE VALUE EQUALING THE PERCENTAGE OF ABSOLUTE VALUE DIVIDING THE AMPLITUDE OF THE CORRESPONDING REFERENCE TRAJECTORY

Subsystem / Reference Input	1st	2nd
Step, $r_{m1}=15, r_{m2}=30$	0.26 (1.7%)	0.46 (1.53%)
Step, $r_{m1}=30, r_{m2}=60$	0.30 (1.0%)	0.50 (0.83%)
Sinusoid Trajectory, $r_{m1}=12, r_{m2}=24, 5Hz$	0.22 (1.83%)	0.47 (1.95%)
Sinusoid Trajectory, $r_{m1}=12, r_{m2}=24, 10Hz$	0.34 (2.83%)	0.58 (2.4%)
Sinusoid Trajectory, $r_{m1}=12, r_{m2}=24, 20Hz$	0.44 (3.6%)	0.84 (3.5%)

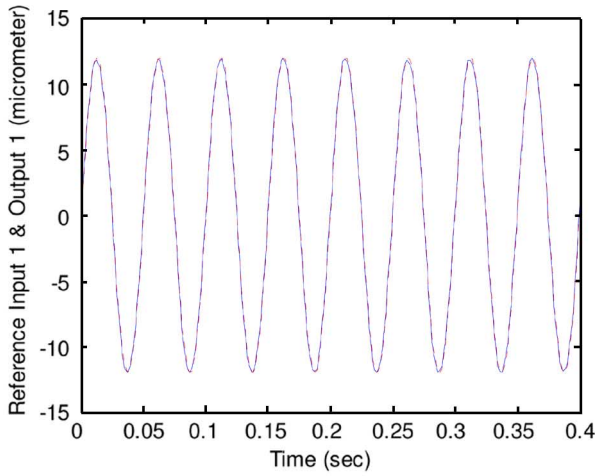

Fig. 7. Output response $(-)$ of the MBFDC for the reference trajectories $R(t) = [\,12\sin(40\pi t) \quad 24\sin(40\pi t)\,]$ μm $(---)$. (a) $r_1(t)$ $(---)$, $y_1(t)$ $(-)$ for $f_1 = 20$Hz, $r_{m_1} = 12\mu$m. (b) $r_2(t)$ $(---)$, $y_2(t)$ $(-)$ for $f_1 = 20$Hz, $r_{m_1} = 24\mu$m.

tracking error will happen. If the frequency of the reference trajectory is not greater than 5 Hz, the maximum steady-state tracking error (i.e., 0.47 μm) is smaller than 2% relative to its amplitude.

To demonstrate the effectiveness of the suggested control, the cases in Figs. 6 and 7 with a 3-kg payload mounted on the X–Y table are scrutinized. These responses are almost the same as that in Figs. 6 and 7. For simplicity, these are not shown. In short, the robust performance of the proposed control for a 2DPDS using the MBFDC is excellent. If $G_1 = I_2$ and $G_2 = 0$, i.e., the CFC, then the system response is oscillatory. Although the oscillation can be reduced by a smaller G_u, its response becomes sluggish. For simplicity, those are omitted.

B. Task Assignment Using the 2DPDS by the MBFDC

In this section, a reference trajectory for a specific motion of the X–Y table [i.e., the dashed line in Fig. 8(a)] is first planned. This specific motion of the X–Y table can be used in the operation of semiconductor manufacture or test. The corresponding reference trajectories for the X-axis and Y-axis (i.e., the dashed lines in Fig. 8(b) and (c), respectively) are obtained. The related response using the proposed control system is shown in Fig. 8, which is satisfactory.

V. CONCLUSION

In this paper, the MBFDC for a 2DPDS is established. The characteristics of the MBFDC for the 2DPDS are summarized as follows. 1) Based on a preload design for the 2DPDS, the system response is improved. 2) No mathematical model for the less-known 2DPDS is required for the controller design. 3) Only the data of system I/O and the information of the upper bound of system knowledge are required for the selection of *five* appropriate control parameters, including two coefficients for the switching surface, two normalizing scaling factors for the switching surface and its derivative, and one output-scaling factor for the crisp control input. 4) The output-scaling factor is determined by the system stability. When a larger output-scaling factor is assigned, a smaller tracking error and a faster response are achieved; however, the risk of transient (or unstable) response happens. 5) The controller design is independent of the reference trajectory, which is not necessary to be a sinusoidal trajectory. 6) Based on our results, the proposed control system can be realized for a micrometer dynamic positioning up to 20 Hz with (or without) the payload. If the frequency of the reference trajectory is not greater than 5 Hz, the maximum steady-state tracking error is smaller than 2% as compared with its amplitude. 7) The proposed control is simple and effective as compared with the PID control and CFC. The proposed control algorithm can be easily implemented in a microprocessor (e.g., DSP of TMS320LF2407).

APPENDIX

Proof of Theorem 1: Define the following Lyapunov function as

$$V(t) = S^T(t)S(t)/2 > 0, \qquad \text{as } S(t) \neq 0. \tag{A1}$$

Authorized licensed use limited to: Tamkang University. Downloaded on June 04,2010 at 03:28:46 UTC from IEEE Xplore. Restrictions apply.

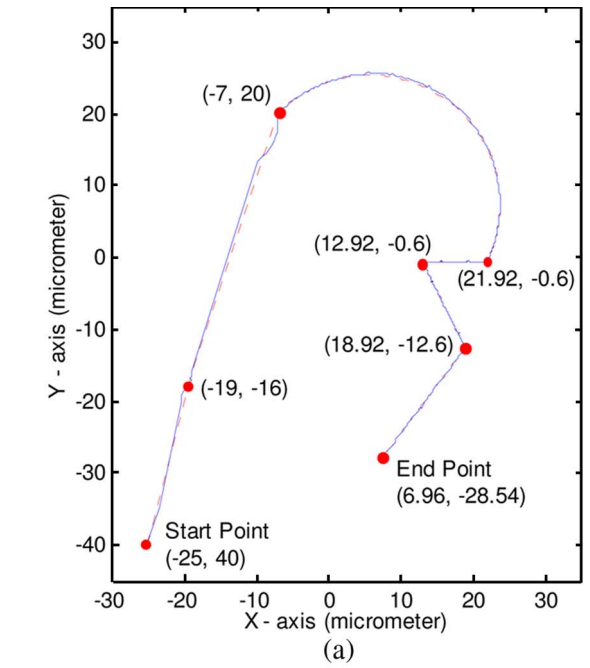

(a)

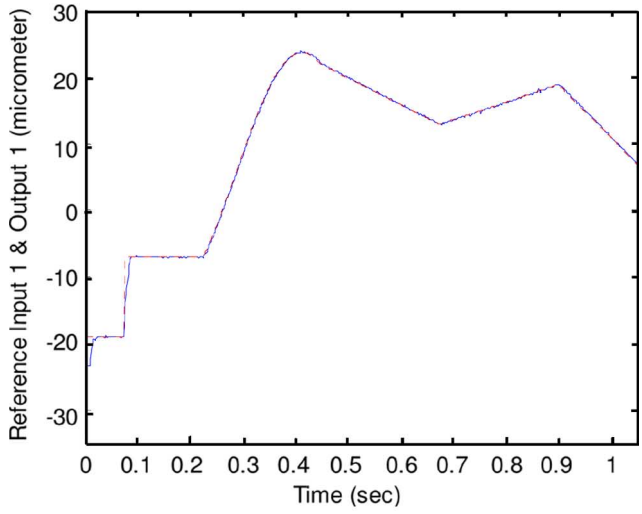

(b)

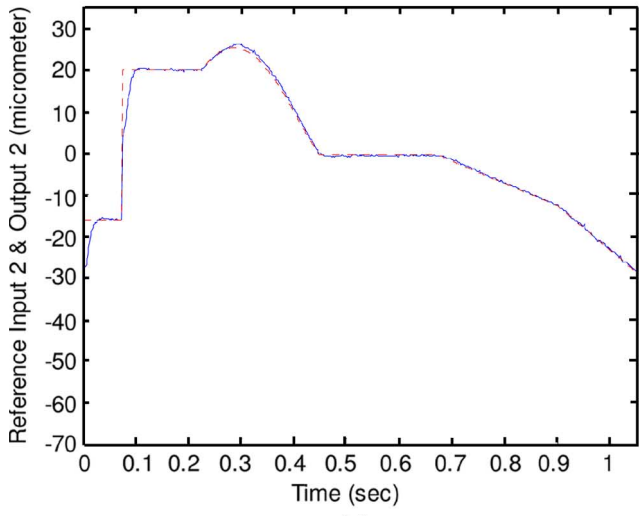

(c)

Fig. 8. Responses of trajectory tracking using the MBFDC. (a) Planning trajectory $(- - -)$ and response of trajectory tracking $(-)$. (b) $r_1(t)$ $(- - -)$, $y_1(t)$ $(-)$ of X-axis. (c) $r_2(t)$ $(- - -)$, $y_2(t)$ $(-)$ of Y-axis.

Taking the time derivative of (A1), substituting (4)–(9) into (A2), and using the fact $G_2A^{-1}C > 0$, yields

$$\begin{aligned}\dot{V} &= S^T\left\{G_1[\dot{R}-\dot{Y}]+G_2\left[\ddot{R}+A^{-1}(B-CU)\right]\right\}\\ &= S^T\left\{H-G_2A^{-1}CU\right\}\\ &= S^TH-S^TG_2A^{-1}CG_u\left[S+\Delta\mathrm{sgn}(S)\right]\\ &\le \|S\|\sum_{i=1}^{2}\{|h_i|-g_{2m}g_{uii}\delta_{ii}/(a_Mc_M)\}\\ &\le -\|S\|\sum_{i=1}^{2}\{\lambda_i\} \le -\lambda\|S\| = -\lambda\sqrt{2V}, \qquad \lambda=\min(\lambda_1,\lambda_2).\end{aligned} \tag{A2}$$

Then, the solution of inequality (A2) for the initial time t_0 and the initial value $S(t_0)$ is described as follows:

$$t - t_0 \le \|S(t_0)\|/\lambda \tag{A3}$$

where t stands for the time that the operating point hits the switching surface (i.e., $S(t) = 0$), and $t - t_0$ denotes the finite time to approach the switching surface. Once the operating point reaches the stable switching surface (4), the tracking error asymptotically converges to zero. ■

ACKNOWLEDGMENT

The author would like to thank the anonymous reviewers for their helpful suggestions that improved the presentation of this paper.

REFERENCES

[1] J. D. Kim and S. R. Nam, "Development of a micro-positioning grinding table using piezoelectric voltage feedback," *Proc. Inst. Mech. Eng. I, J. Syst. Control Eng.*, vol. 209, no. 6, pp. 469–474, 1995.

[2] S. H. Chang, C. K. Tseng, and H. C. Chien, "An ultra-precision $XY\Theta_z$ piezo-micropositioner—Part I: Design and analysis," *IEEE Trans. Ultrason., Ferroelectr., Freq. Control*, vol. 46, no. 4, pp. 897–905, Jul. 1999.

[3] S. H. Chang, C. K. Tseng, and H. C. Chien, "An ultra-precision $XY\Theta_z$ piezo-micropositioner—Part II: Experiments and performance," *IEEE Trans. Ultrason., Ferroelectr., Freq. Control*, vol. 46, no. 4, pp. 906–912, Jul. 1999.

[4] T. Chang and X. Sun, "Analysis and control of monolithic piezoelectric nano-actuator," *IEEE Trans. Control Syst. Technol.*, vol. 9, no. 1, pp. 69–75, Jan. 2001.

[5] N. Bonnail, D. Tonneau, F. Jandard, G. A. Capolino, and H. Dallaporta, "Variable structure control of a piezoelectric actuator for a scanning tunneling microscope," *IEEE Trans. Ind. Electron.*, vol. 51, no. 2, pp. 354–363, Apr. 2004.

[6] E. C. Park, H. Lim, and C. H. Choi, "Position control of $x-y$ table at velocity reversal using presliding friction characteristics," *IEEE Trans. Control Syst. Technol.*, vol. 11, no. 1, pp. 24–31, Jan. 2003.

[7] J. O. Jang, "Deadzone compensation of an xy-positioning table using fuzzy logic," *IEEE Trans. Ind. Electron.*, vol. 52, no. 6, pp. 1696–1701, Dec. 2005.

[8] Z. Z. Lin, F. L. Luo, and M. A. Rahman, "Robust and precision motion control system of linear-motor direct drive for high-speed $x-y$ table positioning mechanism," *IEEE Trans. Ind. Electron.*, vol. 52, no. 5, pp. 1357–1363, Oct. 2005.

Authorized licensed use limited to: Tamkang University. Downloaded on June 04,2010 at 03:28:46 UTC from IEEE Xplore. Restrictions apply.

[9] M. Y. Chen, M. J. Wand, and L. C. Fu, "A novel dual-axis repulsive Maglev guiding system with permanent magnet: Modeling and controller design," *IEEE/ASME Trans. Mechatronics*, vol. 8, no. 1, pp. 77–86, Mar. 2003.
[10] C. J. Li, H. S. M. Beigi, S. Li, and J. Liang, "Nonlinear piezo-actuator control by learning self-tuning regulator," *Trans. ASME, J. Dyn. Syst. Meas. Control*, vol. 115, no. 4, pp. 720–723, Dec. 1993.
[11] P. Ge and M. Jouaneh, "Tracking control of a piezoceramic actuator," *IEEE Trans. Control Syst. Technol.*, vol. 4, no. 3, pp. 209–216, May 1996.
[12] C. L. Hwang, C. Jan, and Y. H. Chen, "Piezomechanics using intelligent variable-structure control," *IEEE Trans. Ind. Electron.*, vol. 48, no. 1, pp. 47–59, Feb. 2001.
[13] R. Perez, J. Agnus, C. Clevy, A. Hubert, and N. Chaillet, "Modeling, fabrication, and validation of a high-performance 2-DOF piezoactuator for micromanipulation," *IEEE/ASME Trans. Mechatronics*, vol. 10, no. 2, pp. 161–171, Apr. 2005.
[14] D. D. Sijak, *Large-Scale Dynamic Systems: Stability and Structure*. Amsterdam, The Netherlands: North Holland, 1978.
[15] R. E. Precup and S. Preitl, "Optimization criteria in development of fuzzy controller with dynamics," *Eng. Appl. Artif. Intell.*, vol. 17, no. 6, pp. 661–674, 2004.
[16] K. Y. Tu, T. T. Lee, and C. H. Wang, "Design of a new fuzzy suction controller using fuzzy modeling for nonlinear boundary layer," *IEEE Trans. Fuzzy Syst.*, vol. 13, no. 5, pp. 605–616, Oct. 2005.
[17] A. Sala, T. M. Guerra, and R. Babuska, "Perspectives of fuzzy systems and control," *Fuzzy Sets Syst.*, vol. 156, no. 3, pp. 432–444, Dec. 2005.
[18] K. Michels, F. Klawonn, R. Kruse, and A. Numberger, *Fuzzy Control: Fundamentals, Stability and Design of Fuzzy Controllers*. Berlin, Germany: Springer-Verlag, 2006.
[19] C. L. Hwang and C. Jan, "Optimal and reinforced robustness designs of fuzzy variable structure tracking control for a piezoelectric actuator system," *IEEE Trans. Fuzzy Syst.*, vol. 11, no. 4, pp. 507–517, Aug. 2003.
[20] E. Tian and C. Peng, "Delay-dependent stability analysis and synthesis of uncertain T–S fuzzy systems with time-varying delays," *Fuzzy Sets Syst.*, vol. 157, no. 4, pp. 544–559, Feb. 2006.
[21] C. L. Hwang, L. J. Chang, and Y. S. Yu, "Network-based fuzzy decentralized sliding-mode control for car-like mobile robots," *IEEE Trans. Ind. Electron.*, vol. 54, no. 1, pp. 574–585, Feb. 2007.
[22] F. Betin, A. Sivert, A. Yazidi, and G. A. Capolino, "Determination of scaling factors for fuzzy logic control using the sliding-mode approach: Application to control a DC machine drive," *IEEE Trans. Ind. Electron.*, vol. 54, no. 1, pp. 296–309, Feb. 2007.
[23] J. Y. Hung, W. Gao, and J. C. Hung, "Variable structure control: A survey," *IEEE Trans. Ind. Electron.*, vol. 40, no. 1, pp. 2–22, Feb. 1993.

Chih-Lyang Hwang (M'95) received the B.E. degree in aeronautical engineering from Tamkang University, Tamsui, Taiwan, R.O.C., in 1981 and the M.E. and Ph.D. degrees in mechanical engineering from Tatung University, Taipei, Taiwan, in 1986 and 1990, respectively.

From 1990 to 2006, he was with the Department of Mechanical Engineering, Tatung University, where he was engaged in teaching and research in the area of servo control and control of manufacturing systems and robotic systems. From 1996 to 2006, he was a Professor of mechanical engineering with Tatung University. From 1998 to 1999, he was a Research Scholar with George W. Woodruf School of Mechanical Engineering, Georgia Institute of Technology, Atlanta. From 2003 to 2006, he was a Member of the Committee in Automation Technology Program of the National Science Council of Taiwan. Since 2006, he has been a Professor in the Department of Electrical Engineering, Tamkang University. He is the author or coauthor of about 100 journal and conference papers in the related field. His current research interests include navigation of mobile robots, fuzzy (or neural-network) modeling and control, variable structure control, robotics, visual tracking systems, and network-based control.

Dr. Hwang received a number of awards, including the Excellent Research Paper Award from the National Science Council of Taiwan and Hsieh-Chih Industry Renaissance Association of Tatung Company. He was a Member of Technical Committee of the 28th Annual Conference of the IEEE Industrial Electronics Society.

Authorized licensed use limited to: Tamkang University. Downloaded on June 04,2010 at 03:28:46 UTC from IEEE Xplore. Restrictions apply.